## RESEARCH ARTICLE

# Low False Alarm and Narrow-Wide Band Compatible Signal Detection Algorithm Combining the Multiscale Wavelet Transform Extremum Detection With the Spectrum Energy Detection

**WEIYING HUANG[1] AND REN WANG [ID]2, (Member, IEEE)**

[1] 10th Research Institute of CETC, Chengdu 610036, China

[2] Institute of Applied Physics, University of Electronic Science and Technology of China, Chengdu 610054, China

Corresponding authors: Weiying Huang (huangweiying@cetc.com.cn) and Ren Wang (rwang@uestc.edu.cn)

**ABSTRACT** A low false alarm and narrow-wide band compatible signal detection algorithm is proposed by combining the multiscale wavelet transform extremum detection with the spectrum energy detection. The signals with different bandwidths are detected at respective wavelet scales. Signal detection at a single scale adopts the detection strategy of combining the wavelet transform extremum detection with the spectrum energy detection to decrease the probability of detecting spurious signals caused by noises, and the noise floor estimation and spectrum modification are completed by morphological filtering to solve the problem of the noise floor fluctuation. Finally, the detection results at multiple scales are fused and eliminated selectively. The simulation results show that the proposed algorithm is able to achieve excellent narrow-wide band compatible detection performance while realizing a relatively low probability of detecting spurious signals.

**INDEX TERMS** Signal detection, multiscale wavelet transform, spectrum energy detection, morphological filtering.

## I. INTRODUCTION

Signal detection is the primary task of the signal reconnaissance and the basis of the signal analysis [1], [2], [3], [4], [5], [6]. Early classical signal detection techniques, including the energy detection(ED), matched-filter detection (MFD), and cyclic stationary feature detection (CFD), are proposed for narrow-band systems [7], [8], [9]. With the improvement of electronic devices, the bandwidth of the reconnaissance receiver increases, therefore, wideband signal detection techniques have attracted much attention [10], [11], [12], [13], [14].

The associate editor coordinating the review of this manuscript and approving it for publication was Vicente Alarcon-Aquino [ID].

Dividing the wideband spectrum into multiple sub-bands and detecting signals in each sub-band respectively with narrow-band signal detection algorithms is a conventional wideband signal detection method [15], [16], [17], [18]. In [16], the wideband spectrum is filtered to multiple narrow-band spectrums with a set of filters in parallel and detected in each band concurrently. A sweep tune detection technique is introduced in [18], where a local oscillator signal, whose frequency is swept sequentially over the frequency range of interest, is mixed with the wideband signal for the signal detection. However, the hardware cost and time cost of the mentioned conventional methods are contradictory. In other words, either the front-end hardware configuration is complex or a long time is required to scan the entire wide frequency range, resulting in the detection probability

decrease of burst signals. Moreover, the prior information for sub-band division must be provided. In recent years, compressed sensing has been used for wideband signal detection [19], [20], [21], [22], [23], which can effectively reduce the sampling rate requirement and simplify the hardware complexity of the front-end. However, the spectrum of the compressed sensing based wideband signal detection should be sparse in nature, which may be unsatisfied in the actual environment.

The wideband signal detection can be seen as a spectral edge detection problem. Wavelet analysis is an effective mathematical tool for analyzing signal singularity, which has been proved to be a reliable technique for the spectral edge detection with less hardware and time costs, more spectrum flexibility and no prior knowledge [24], [25], [26], [27], [28], [29], [30], [31], [32]. Several wavelet transform based methods have been researched for spectral edge detection [27], [28], [29], [30], [31], [32], [33], [34], [35], [36], [37], [38], [39], [40], [41], [42], [43]. Among these methods, the wavelet transform multiscale product (WTMP) and wavelet transform multiscale sum (WTMS) algorithms were widely used due to the suppression of spurious local modulus maxima caused by noise. The WTMP realizes the edge detection through detecting the local modulus maxima of the WTMP [33], [34], [35], [36], [37], [31], [38], [39], [40]. It suppresses the spurious local modulus maxima caused by noise and enhances the local modulus maxima corresponding to the signal edges through the multiplication operation. However, when extremely narrow-band signals and wide bandwidth signals need to be detected simultaneously, one of them may be suppressed [40], which would cause the decrease of probability of detection. Compared to the WTMP, WTMS retains the information about the signal at all scales and avoids the signal suppression caused by multiscale multiplication [40], [41], [42], [43]. However, the denoising effect of the WTMS is worse than WTMP, thus the probability of detecting spurious signals is much higher than that of WTMP and needs to be further lowered. Therefore, lowering the probability of detecting spurious signals while ensuring high narrow-wide band compatible detection probability is a challenge.

In this paper, a low false alarm and narrow-wide band compatible signal detection algorithm is proposed by combining the multiscale wavelet transform extremum detection with the spectrum energy detection. The narrowband signals and wideband signals within the frequency range of interest are detected at the small and large dyadic scales respectively. The proposed algorithm adopts the signal detection strategy of combing the wavelet transform local extreme detection with the spectrum energy detection at a single scale, which could effectively reduce the detection of spurious signals caused by noise. In addition, the effects of the spectrum noise floor fluctuation are considered. The morphological filtering is applied to estimate the noise floor and modify the wideband spectrum to avoid the miss-detection of signals in

the trough position of the spectrum and the false alarm of strong noises at the peak, caused by the un-flat noise floor. At last, signal detection results at multiple scales are fused and eliminated selectively to further reduce false alarm. The proposed algorithm is compared with signal detection algorithms based on WTMP and WTMS by MATLAB simulation. The simulation results show that the proposed algorithm has better detection performance among the whole SNR range compared to the signal detection algorithm based on WTMP. Although its detection performance is similar to that of the signal detection algorithm based on WTMS at SNRs above 5dB, it outperforms the signal detection algorithm based on WTMS at low SNRs 0-5dB. In terms of performance of rejecting the spurious signals, the proposed algorithm is superior to signal detection algorithm based on WTMS. In summary, the proposed algorithm successfully lowers the probability of detecting spurious signals on the premise of ensuring high narrow-wide band compatible detection probability.

The rest of the paper has been organized as below. The design process of the algorithm is represented in detail in Section II, the performance simulations and analyses are discussed in Section III, and the conclusion of the paper is drawn in Section IV.

## II. DESIGN OF THE PROPOSED ALGORITHM

Suppose that the frequency range for the wideband signal detection is $[f_{start}, f_{end}]$ and the detection bandwidth is denoted as $BW$. The frequency range contains $N$ signals, whose center frequencies and bandwidths are represented as $\{f_n\}_{n=1}^N$ and $\{B_n\}_{n=1}^N$, respectively. We adopt the following assumptions:

• The frequency range of interest $[f_{start}, f_{end}]$ and detection bandwidth $BW$ are known;

• The number of signals $N$, the center frequency $\{f_n\}_{n=1}^N$ and bandwidths $\{B_n\}_{n=1}^N$ are unknown to the cognitive radio receiver;

• The ambient noise is additive Gaussian white noise whose two-side power spectrum density is denoted as $S_w(f) = {N_0}/{2}, \forall f$.

The purpose of wideband signal detection is to obtain the number of signals $N$ and related signal parameters $\{f_n\}_{n=1}^N$, $\{B_n\}_{n=1}^N$. The overall design diagram of the algorithm is shown in Figure 1. Firstly, the power spectrum density (PSD) is computed through fast Fourier transform (FFT) and intercepts spectral data corresponding to the detection frequency band $[f_{start}, f_{end}]$, expressed as $S(n), n = 0, 1, \ldots, L-1$, $L$ indicates the wideband spectrum length. Then, different wavelet transform scales are selected, the wavelet transform of the wideband spectrum is performed at each scale and the signals are detected at each scale. Finally, the signal detection results are obtained by merging the signals detected repeatedly at multiple scales and eliminating selectively the false signals. The detailed processes are elaborated as following.
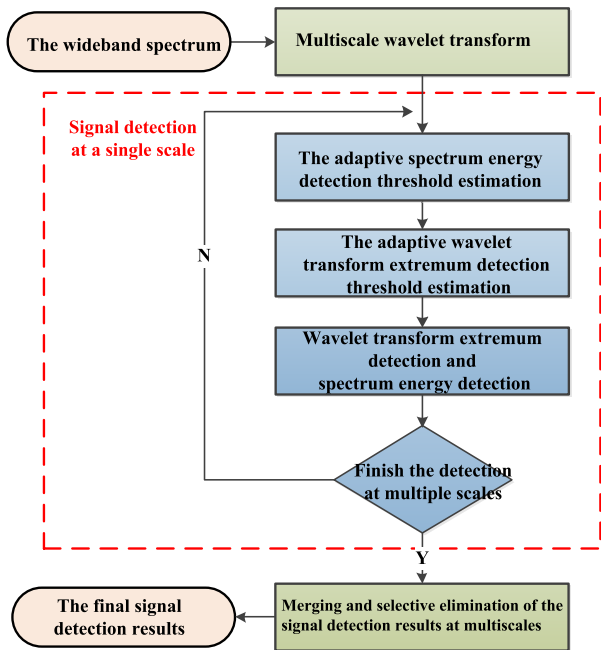
**FIGURE 1.** Overall design block diagram of the algorithm.

## A. SELECTION OF WAVELET BASIS FUNCTION AND WAVELET SCALES

The cubic B-spline basis function is chosen as the smoothing function because the cubic B-spline wavelet is asymptotically optimal in the edge extraction [25]. Denote the cubic B-spline basis function as $\Omega_4(t)$, as shown in Equation (1), the mother wavelet function $\psi(t)$ is $\psi(t) = (\Omega_4(t))'$.

$$\Omega_4(t) = \begin{cases} -\dfrac{|t|^3}{6} + t^2 - 2|t| + \dfrac{4}{3}, & 1 < |t| < 2 \\ \dfrac{|t|^3}{2} - t^2 + \dfrac{2}{3}, & |t| \leq 1 \\ 0, & |t| \geq 2 \end{cases} \quad (1)$$

Because the continuous wavelet transform is redundant, the dyadic discrete wavelet transform (DWT) is used in the proposed algorithm. Denote the wavelet transform coefficient of $x(t)$ at scale $2^j$ as $d_j(t)$, the wavelet coefficients can be calculated by

$$d_j(t) = \left\langle x(t) \,|\, \psi_{2^j}(t) \right\rangle \quad (2)$$

where $\psi_{2^j}(t) = \frac{1}{\sqrt{2^j}} \psi\left(\frac{t}{2^j}\right)$ is the wavelet basis function at scale $2^j$, $\langle a|b \rangle$ represents the inner product of $a$ and $b$.

According to the multi-resolution analysis principle of the wavelet transform, at small scales, the wavelet transform coefficients of some wideband signals with slow-variated spectral edges are small because the smoothing interval for signals is small, which results in the miss-detection of wideband signals. It is suitable for the detection of narrowband signals. On contrary, at large scales, the smoothing interval for signals is large, which results in the narrow-band signals being smoothed and miss-detected. It is suitable for the detection of wideband signals with slow variated edges. Therefore,

the multiscale comprehensive analysis is required in detecting signals with different bandwidths.

As mentioned above, the transform scales are determined by the signal bandwidth. Assuming that the sampling rate is $f_s$, frequency resolution is $\Delta f$ and spectrum length is $L$. Because the bandwidth range of the signal to be detected can not be predicted in advance, in order to ensure no miss-detection, the bandwidth range of $\Delta f \sim f_s/2$ is fully considered. The signal bandwidth can be divided by order of magnitude, as shown in Figure 2, these numbers represent the number of spectrum points corresponding to the signal bandwidth. Actual bandwidth range $B_s$ and recommended wavelet scales corresponding to the spectrum point division are given as Table 1.
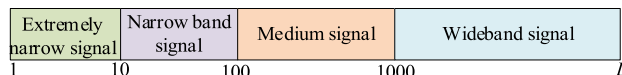


**FIGURE 2.** Signal bandwidth division by order of magnitude.

**TABLE 1.** The wavelet scales corresponding to different bandwidths.

| Signal Type | Bandwidth range $B_s$ | Wavelet scale $j$ |
|---|---|---|
| extremely narrow signal | $\Delta f \leq B_s \leq 10\Delta f$ | 4 |
| narrowband signal | $10\Delta f \leq B_s \leq 100\Delta f$ | 6 |
| medium signal | $100\Delta f \leq B_s \leq 1000\Delta f$ | 8 |
| wideband signal | $1000\Delta f \leq B_s \leq f_s/2$ | 10 |

## B. DESIGN OF THE SIGNAL DETECTION ALGORITHM AT A SINGLE SCALE

The wideband signal detection can be attributed to the spectral edge detection corresponding to the boundaries of signals. The edge detection problem can be transformed into the wavelet transform extremum detection, where the rising edges and descending edges of the signal correspond to the local wavelet transform maximum value and minimum value [25], respectively. However, the burrs of the noise floor will cause the generation of spurious wavelet extremes. When the wavelet transform extremum detection threshold is low, serious false alarms or false detections would arise, especially at small scales. Therefore, the algorithm formulates a detection strategy that combines the spectrum energy detection with the wavelet transform extremum detection to reduce false alarms, false detections, and missed detections. The wideband signal detection algorithm at a single scale would be introduced from three aspects: the noise floor and spectrum energy detection threshold estimation, the adaptive wavelet transform extremum detection threshold estimation, and the detection strategy.

### 1) THE NOISE FLOOR AND SPECTRUM ENERGY DETECTION THRESHOLD ESTIMATION

The energy detection threshold estimation is the key of the spectrum energy detection. Due to the complexity of

the external electromagnetic environment and the influence of RF front-end receiving equipment, the noise floor of the wideband spectrum may be uneven. If a fixed energy detection threshold is adopted directly, it will cause the miss-detection of the weak signal at the trough of the spectrum curve and the false alarm of strong noises at the peak. To solve this problem, the algorithm first performs morphological filtering operation on the wideband spectrum to estimate the noise floor and modify the spectrum. Then, the threshold estimation value of energy detection is calculated adapting to the modified spectrum.

Suppose $f(x)$ is a discrete sequence defined on $Z^n$, the structural element $B$ is a finite subset of $Z^n$, and $B^s = \{-b : b \in B\}$ is a symmetric set of $B$ about the origin, $B_x = \{b + x, b \in B^s, x \in Z^n\}$ is the translation about $B^s$. Four basic morphological transformations can be described as below: The dilation and erosion operations of $f(x)$ with respect to $B^s$ are defined respectively:

$$(f \oplus B^s)(x) = \max_{b \in B_x} \{f(b)\}, \tag{3}$$

$$(f \odot B^s)(x) = \min_{b \in B_x} \{f(b)\}, \tag{4}$$

The opening and closing operations of $f(x)$ with respect to $B^s$ are defined respectively:

$$(f \circ B^s)(x) = \left[(f \odot B^s) \oplus B^s\right](x) = \max_{a \in B_x} \left\{ \min_{b \in B_a} \{f(b)\} \right\}, \tag{5}$$

$$(f \bullet B^s)(x) = \left[(f \oplus B^s) \odot B^s\right](x) = \min_{a \in B_x} \left\{ \max_{b \in B_a} \{f(b)\} \right\}, \tag{6}$$

where $B_a = \{b + a, b \in B^s, a \in Z^n\}$ is the translation about $B^s$.

The processes of the adaptive energy detection threshold estimation are described as following:

1) Perform the mean smoothing on the input wideband spectrum $S(n), n = 0, 1, \ldots, L-1$ and obtain the smoothed spectrum $S_1(n), n = 0, 1, \ldots, L-1$;

2) Use the linear structural element $B^s$ to perform an opening operation on the spectrum $S_1(n)$ to obtain the noise floor estimation $N_1(n), n = 0, 1, \ldots, L-1$;

3) Subtract $N_1(n)$ from the spectrum $S_1(n)$ to obtain the modified spectrum $S_2(n), n = 0, 1, \ldots, L-1$;

4) Perform the closing operation on the spectrum $S_2(n)$ to obtain the top estimate of noise $N_2(n), n = 0, 1, \ldots, L-1$, and cluster $N_2(n)$ to get the adaptive energy detection threshold, expressed as $thr0$.

### 2) ADAPTIVE WAVELET TRANSFORM EXTREMUM DETECTION THRESHOLD ESTIMATION

If the wavelet transform coefficients are divided into bins with a uniform width, the statistical distribution of the coefficients has the characteristics that the number of the coefficients in the bin close to 0 has the largest proportion, and the proportion of the number of the coefficients in the bin far

from 0 gradually decreases. For example, the wavelet transform coefficients of a wideband spectrum and its statistic histogram are shown in Figure 3. The rising edge and descending edge threshold of the adaptive wavelet transform extremum detection, respectively denoted as $thr1$ and $thr2$, can be estimated based on the statistic distribution characteristics.
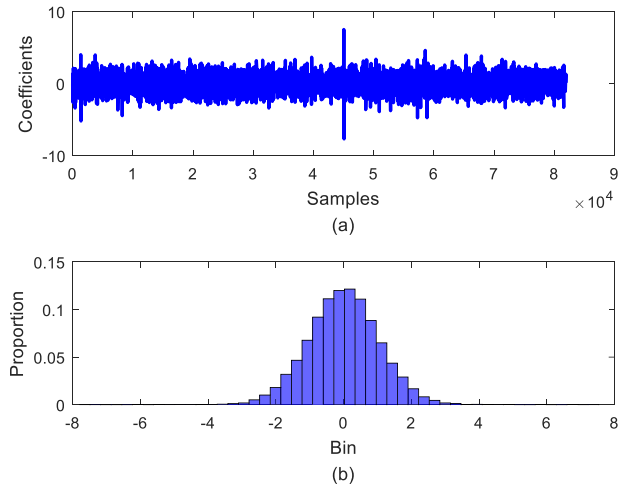


**FIGURE 3.** Statistical distribution characteristic of the wavelet transform coefficients: (a) The wavelet transform coefficients; (b) The Statistical distribution histogram.

Firstly, the wavelet transform coefficients are divided into equally spaced bins according to the maximum and minimum values of the coefficients. Then, count the number of coefficients that fall in each bin and calculate their relative proportions to all coefficients. Next, accumulate the proportion in order from high to low. When the accumulated value is greater than the accumulation threshold which is set as 0.9, the accumulation is terminated. The wavelet transform coefficients in the bin at the time of termination are averaged to obtain the average value $thd$. If $thd$ is greater than 0, $thr1 = thd$ and $thr2 = -thd$, otherwise $thr2 = thd$ and $thr1 = -thd$.

### 3) SIGNAL DETECTION STRATEGY AT A SINGLE SCALE

In order to decrease the probability of detecting spurious signals caused by noises, the algorithm combines the wavelet transform extremum detection with the spectrum energy detection to realize the signal detection at a single scale. Assume that wavelet coefficients are expressed as $d_j(n), n = 0, 1, \ldots, L-1$, $L$ is the length of wideband spectrum as mentioned before. Firstly, the signal edge detection is executed point by point on $d_j(n)$, according to $thr1$ and $thr2$. Mathematically, the detection condition of the signal edges can be described as below:

• When the detection condition $(d_j(n) > thr1) \,\&\&\, (d_j(n + n_{ring\_continuos}) < thr1)$ is satisfied, the left edge $n_{sig\_start}$ of the signal is denoted by $n_{sig\_start} = n_{\max\_local}, d(n_{\max\_local}) = \max(d(n : n + n_{ring\_continuos}))$.

• When the detection condition $(d_j(n) < thr2) \,\&\&\, (d_j(n + n_{descend\_continuous}) > thr2)$ is satisfied, the right

edge $n_{sig\_end}$ of the signal is denoted by $n_{sig\_end} = n_{\min\_local}, d(n_{\min\_local}) = \min\left(d(n : n + n_{descend\_continuous})\right)$.

After detecting the edges of the signal, we need to judge whether the signal corresponding to the frequency position range $[n_{sig\_start}, n_{sig\_end}]$ is valid. We define the proportion of points above the energy detection threshold $thr0$ within the signal boundaries as

$$ra = \frac{N_{sum}}{n_{sig\_end} - n_{sig\_start} + 1}, \qquad (7)$$

where $N_{sum}$ is the number of the points which satisfy $\{S_2(n) > thr0, n \in [n_{sig\_start}, n_{sig\_end}]\}$, $S_2(n)$ is the modified wideband spectrum. If $ra$ is greater than the ratio threshold, the signal is determined as a valid signal. The setting of the ratio threshold needs to consider the spectral fluctuations within the signal bandwidth. An example of the signal detection strategy at a single scale is shown in Figure 4.
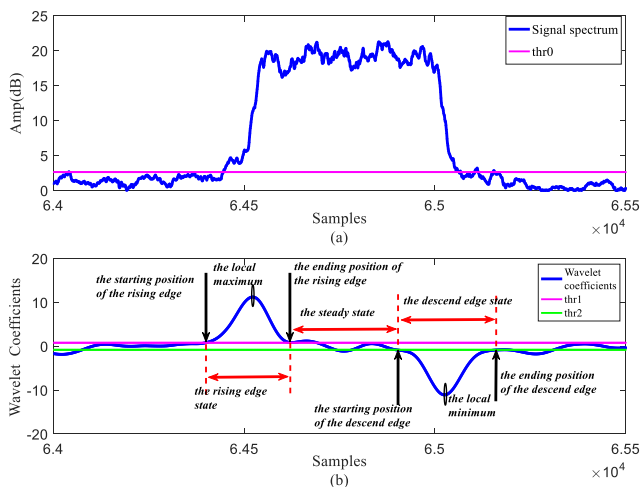


**FIGURE 4.** An example of the signal detection strategy at a single scale: (a) The spectrum energy detection; (b) The wavelet transform extremum detection.

The specific algorithm processing flow chart is shown in Figure 5. The parameters of each detected signal include the starting and ending position of the signal, the position of the signal center frequency, bandwidth, and amplitude of the signal.

## C. MERGING AND SELECTIVE ELIMINATION OF THE SIGNAL DETECTION RESULTS AT MULTIPLE SCALES

For the signal detection results at multiple scales, there are some problems:

- One signal may be detected repeatedly at more than one scale;
- Partial areas of wideband signal may be detected as the narrowband signals at a small scale because of the fluctuation within signal bandwidth. An example is shown in Figure 6, three narrowband signals are falsely detected within the wideband signal at scale $2^6$;
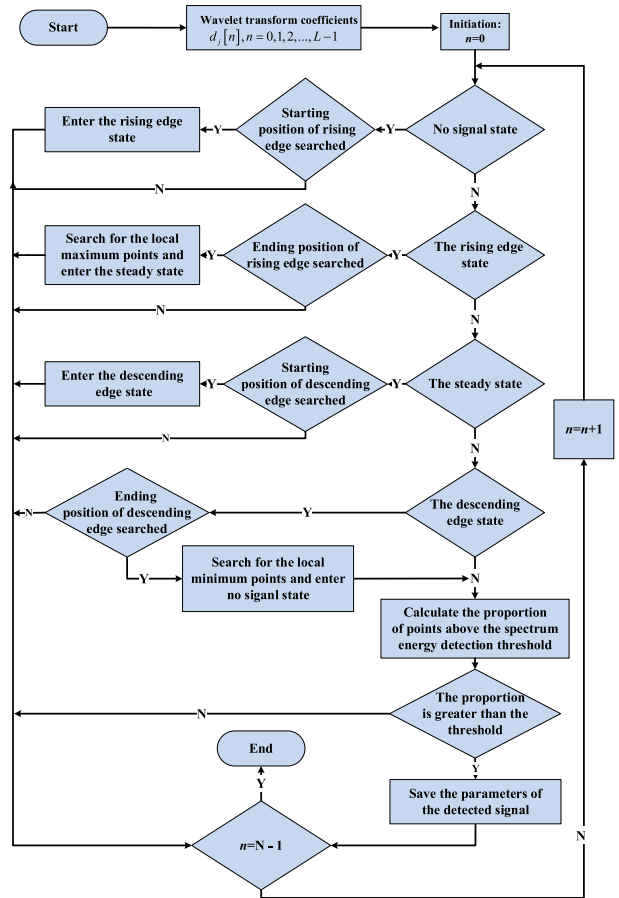- Multiple signals closely spaced may be detected as a wideband signal at a large scale. An example is shown



**FIGURE 5.** The flowchart of the signal detection strategy at a single scale.

in Figure 7, ten narrowband signals are detected as one wideband signals at scale $2^{10}$.

Therefore, it is necessary to merge and eliminate selectively the signal detection results at different scales. The algorithm merges two signals detected repeatedly at the adjacent scales according to the space of two signals' center frequency positions. Then the merged detection results of two scales are eliminated selectively based on the overlapping rate to retain the wideband signals or narrowband signals. The merging and elimination operations start from the first scale and the second scale. The signal detection results after merging and eliminating are reserved to repeat the above process with the next scale until the detection results of all scales are processed. The design block diagram is shown as Figure 8.

Assume that the signal detection results at two scales are defined by $D_1[m]$, $m = 0, 1, 2\ldots, m_1 - 1$ and $D_2[n]$, $n = 0, 1, 2\ldots, n_1 - 1$, respectively, where $m_1, n_1$ represent the number of the signals detected at two scales. The merged results are stored in set $U$. The merging and selective elimination processes of the detection results at two scales are given below.

1. $m, n$ are both initiated as 0.

2. Calculate the absolute difference of the signal center frequency positions of $D_1[m]$ and $D_2[n]$, denoted by $d$, and
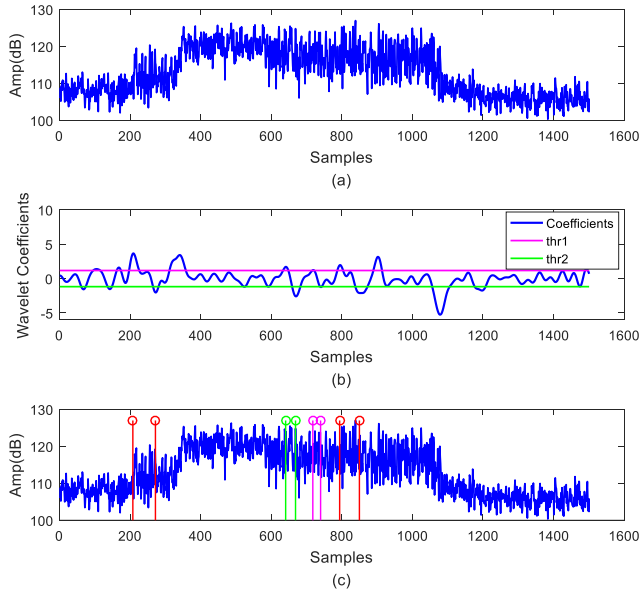
**FIGURE 6.** An example of partial areas of a wideband signal being detected as three narrowband signals at a small scale: (a) The spectrum of a wideband signal; (b) The wavelet transform coefficients of the signal in (a) at scale $2^6$; (c) The detection results at scale $2^6$.
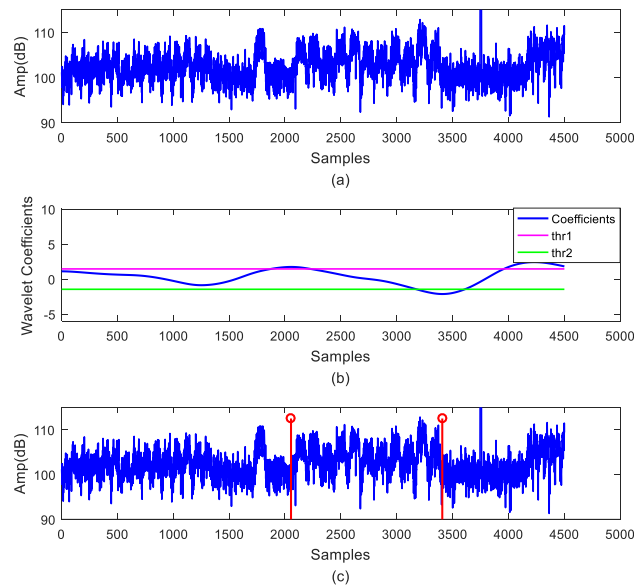


**FIGURE 7.** An example of multiple signals closely spaced being detected as a wideband signal at a large scale: (a) The spectrum containing multiple signals; (b) The wavelet transform coefficients of the signals in (a); (c) The detection results at scale $2^{10}$.

calculate the ratios of the overlapping parts of the two signals to their respective signal bandwidths, and take the larger one, defined by $r$.

3. Merging condition judgement: if $d$ is less than the center frequency position difference threshold $d\_thr$ which is set as 0.15 times of the larger bandwidth points, $D_1[m]$ and $D_2[n]$ are merged and store the signal with smaller bandwidth to $U$, then go to Step 5, otherwise go to Step 4.

4. Set $n = n + 1$, if $n > n_1 - 1$, store $D_1[m]$ to $U$ and go to Step 5, otherwise go back to Step 2.

5. Set $m = m + 1, n = 0$, if $m > m_1 - 1$, go to Step 6, otherwise go back to Step 2, and it should be noted that when Step 2 is executed, the signals detected at the second scale that have been stored in $U$ should be skipped.

6. Store the detected signals that have not been merged at the second scale to $U$.

7. Signal set $U$ is divided into a wide bandwidth signal set $X$ and a narrow bandwidth signal set $Y$ according to the signal bandwidth points threshold $bw\_thr$, which is set as 100.
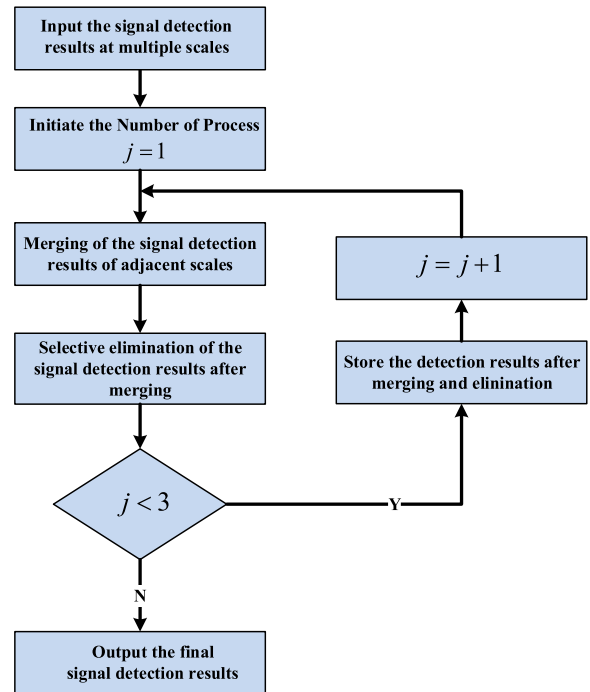


**FIGURE 8.** Design block diagram of the merging and elimination of multiscale signal detection results.

8. For each signal $s$ in the set $X$, sum the spectrum points of the signals, which are included within the bandwidth of the signal $s$, in the set $Y$, and calculate the proportion of the sum of the included parts to $s$, expressed by $r1$. If $r1$ is larger than overlapping ratio threshold $r\_thr2$ which is set as 0.5, retain the multiple narrowband signals within the bandwidth of $s$ and delete $s$, otherwise retain $s$ and delete the multiple narrowband signals.

9. Perform another round of selective elimination in the reserved wideband signals of Step 8 to obtain the final signal detection result.

## III. PERFORMANCE EVALUATION OF THE ALGORITHM
### A. PERFORMANCE MEASURES

As mentioned in [44], the wideband frequency range has been pre-defined to multiple bands and they are perfect prior knowledge for the conventional wideband signal detection methods. They can be described as a classical binary hypothesis testing problem for each band (also called multiband

detection problem). Mathematically, this is denoted by:

$$H_{0,m} : \boldsymbol{y}_m = \boldsymbol{v}_m, \quad m = 1, 2, \ldots, M, \tag{8}$$

$$H_{1,m} : \boldsymbol{y}_m = \boldsymbol{x}_m + \boldsymbol{v}_m, \quad m = 1, 2, \ldots, M, \tag{9}$$

where $\boldsymbol{y}_m$ is the received signal at the receiver, $\boldsymbol{x}_m$ is the transmitted useful signal, $\boldsymbol{v}_m$ is the white Gaussian noise, $m$ represents the sub-band number, $M$ represents the total number of sub-bands. In this case, for each sub-band, one crucial element is to define a proper test statistic to differentiate the two hypotheses $H_{0,m}$ and $H_{1,m}$, another vital element is the set of decision threshold. The performance can be evaluated by the detection probability $P_d$ and false alarm probability $P_{fa}$. The receiver operating characteristic (ROC) curve is a classic performance metric for a binary classification problem. When the decision threshold is varied, we can get a series of $P_d$ and $P_{fa}$ and plot the ROC curve.

However, in practice, cognitive radio network must be able to support heterogeneous transmission schemes (signal frequency, bandwidth, modulation type, etc.), thus the center frequencies and bandwidths of the signals that need to be detected in the wideband spectrum are unknown. In other words, there is no prior information of bands for wideband signal blind detection based on edge detection and it is not equivalent to a binary hypothesis testing problem.

There are also some researches that convert the wideband signal detection based on wavelet transform edge detection into a binary hypothesis testing problem. In [32] and [39], divide the spectrum into sub-bands according to the detected edges and determine the existence of signal within each band. Then, the wideband signal detection is formulated as a statistical hypothesis testing problem for each sub-band. However, they are both based on the assumption that the wideband spectrum is composed by a set of successive frequency sub-bands which are flat within the bands, as such irregularities in the wideband spectrum only appear at the edges of these sub-bands. The assumption is not valid in actual situation. There may be sharp changes within signal bands and noise section of the spectrum such that errors in the detection of the edges are possible and the detection accuracy of edges itself is an important performance metric.

Thus, the conventional metric such as the false alarm probability is not valid for the performance assessment of the wideband signal detection based on wavelet transform edge detection. New performance measures are needed to be defined to assess the ability of detecting signals correctly and reject the spurious signals caused by noise in wideband spectrum [43], [44], [45].

In this paper, we define variables $P_c$ and $P_f$ to assess the algorithm performance. It is assumed that the number of signals that exist actually in the wideband spectrum denotes as $N_{sig}$, the number of signals that are correctly detected denotes as $\widetilde{N}_{sig}$, the total number of signals that are detected

is $\widetilde{N}_{\det ected}$, we define

$$P_c = \frac{\widetilde{N}_{sig}}{N_{sig}}, \tag{10}$$

$$P_f = \frac{\widetilde{N}_{\det ected} - \widetilde{N}_{sig}}{\widetilde{N}_{\det ected}}, \tag{11}$$

$P_c$ represents the ratio of the number of correctly detected signals to the total number of actual signals. It is used to evaluate the algorithm performance of detecting signals correctly. $P_f$ represents the ratio of the number of falsely detected signals to the total number of signals that are detected. It is used to assess the algorithm performance of rejecting the false signals caused by noise and reflects the accuracy of detection.

### B. PERFORMANCE SIMULATIONS OF THE ALGORITHM

As usual, the receiver downconverts the radio frequency wideband signal to a fixed intermediate frequency (IF) wideband signal and then sends it to the detection block. Without loss of generality, it is assumed that the receiver bandwidth is 60MHz and the intermediate frequency range of detecting signals is [22 82] MHz, which refers to the reconnaissance frequency range and reconnaissance bandwidth of the IF receiver commonly used in our engineering projects. Power spectrum density (PSD) of the IF wideband signal is computed through fast Fourier transform (FFT). The size of FFT is set to 262144 to ensure excellent frequency resolution accuracy.

#### 1) SIMULATION ANALYSES OF THE FEASIBILITY OF THE ALGORITHM FOR SIMULTANEOUS DETECTION OF THE NARROWBAND AND WIDEBAND SIGNALS

A set of simulation analyses are conducted to demonstrate the feasibility of the proposed algorithm for simultaneous detection of the narrowband and wideband signals with different SNRs. In the setting of simulation conditions shown in Table 2, there are ten signals which are all the binary phase shift keying (BPSK) modulated signals with a rolling down coefficient of 0.35. The frequencies of the signals are randomly selected within the detection bandwidth range [22 82] MHz. These signals have five different symbol rates and two SNRs for each symbol rate. Furthermore, due to the complexity of the external electromagnetic environment

**TABLE 2.** Simulation parameter settings for demonstrating the feasibility of simultaneous detection of the narrowband and wideband signals.

| Index of signal | 1 | 2 | 3 | 4 | 5 | 6 | 7 | 8 | 9 | 10 |
|---|---|---|---|---|---|---|---|---|---|---|
| Symbol rate/Ksps | 30 | 400 | 200 | 250 | 800 | 30 | 400 | 200 | 250 | 800 |
| IF frequency /MHz | 23 | 25 | 30 | 35 | 45 | 55 | 58 | 65 | 70 | 80 |
| SNR/dB | 7 | 7 | 7 | 7 | 7 | 12 | 12 | 12 | 12 | 12 |

and the influence of RF front-end receiving equipment, the noise floor of the wideband spectrum may be uneven in real situations. This case is considered in the simulation condition setting, slow-changing noise fluctuations with maximum 5dB have been added artificially in the receiving band except for the additive Gaussian white noise. The spectrum within the receiving band is shown in Figure 9.
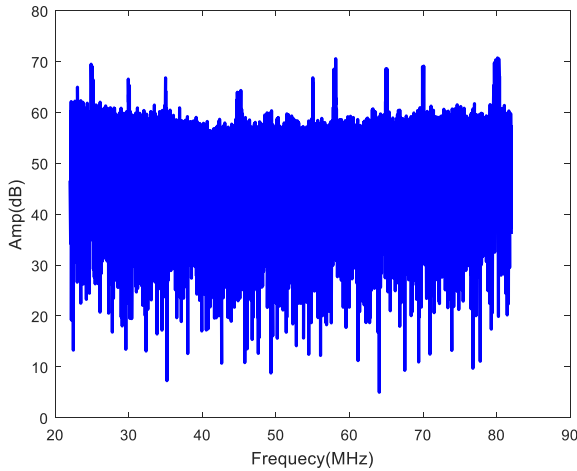


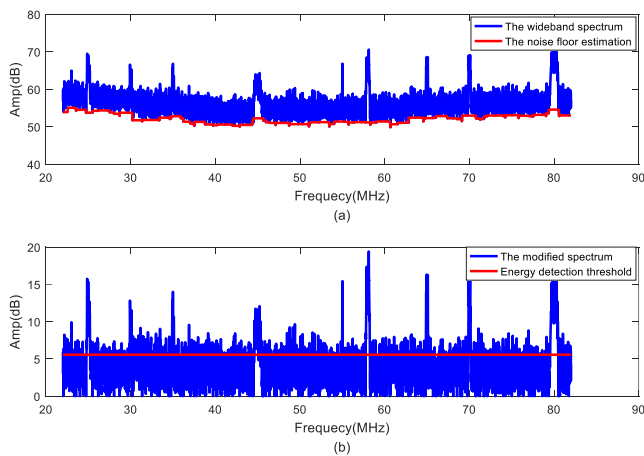**FIGURE 9.** A wideband spectrum within the receiving band.



**FIGURE 10.** The adaptive spectrum energy detection threshold estimation: (a) The noise floor estimation; (b) the modified spectrum and energy detection threshold estimation.

The simulation of the spectrum energy detection threshold estimation is shown in Figure 10. Figure 10(a) shows the noise floor estimation result of the spectrum after the mean smoothing, in which the red curve is the noise floor estimation. Figure 10(b) shows the spectrum modified according to the noise floor estimation and the red line is the estimation value of the spectrum energy detection threshold. It can be seen from Figure 10, the noise floor estimate fits the real noise bottom curve well and the modified spectrum removes the noise floor fluctuation. Through the estimation and clustering of the noise top of the modified spectrum, the adaptive energy detection threshold estimation value is obtained.
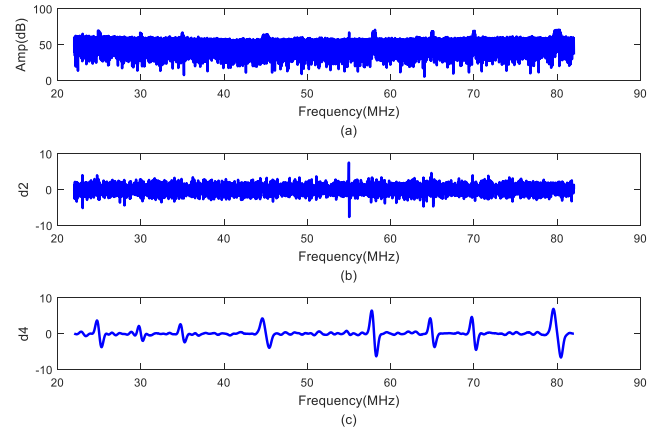


**FIGURE 11.** Wavelet transform of wideband spectrum at different scales: (a) The wideband spectrum; (b) The wavelet transform at scale $2^6$; (c) The wavelet transform at scale $2^{10}$.

The wavelet transform of the wideband spectrum at scale $2^6$ and $2^{10}$ are shown in Figure 11. It can be found that the extreme values of the wavelet transform corresponding to the edge of the narrowband signal are obvious at small-scale transform, while the extreme values of the wavelet transform corresponding to the edges of the wideband signal are obvious at the large-scale transform. This is consistent with multi-resolution analysis theory of the wavelet transform.

The final signal detection results after merging and selective elimination are shown in Figure 12. Figure 12(a) marks the signals existing in the wideband spectrum, and Figure 12(b) shows the results of the signal detection algorithm, vertical lines indicate the starting and ending boundary positions of the detected signals, in which different colors represent different signals. Compared Figure 12(a) with Figure 12(b), it can be seen that the proposed algorithm could detect signals with narrow bandwidth, such as numbered 1 and 6 in Figure 12(a), and signals with wide bandwidth, such as signals numbered 5 and 10 in Figure 12(a). In other words, the algorithm is compatible with the detection of wide and narrow bandwidth signals at the same time.

### 2) PERFORMANCE SIMULATION ANALYSES OF THE ALGORITHM AT DIFFERENT SNRs

In order to demonstrate the influence of the SNR on the performance of the algorithm, the algorithm performance at different SNRs are analyzed through multiple Monte Carlo simulations and compared with other signal detection methods based on WTMP and WTMS, respectively. The detailed simulation parameter settings are listed in Table 3. As shown in Table 3, 500 Monte Carlo simulations are executed for each SNR. Ten BPSK modulated signals are generated in each Monte Carlo simulation, the frequencies of the signals are randomly generated within the detection bandwidth range [22 82] MHz, as long as these signals do not overlap in the frequency domain. The symbol rates of the signals are generated randomly within a wide range [30 800] Ksps
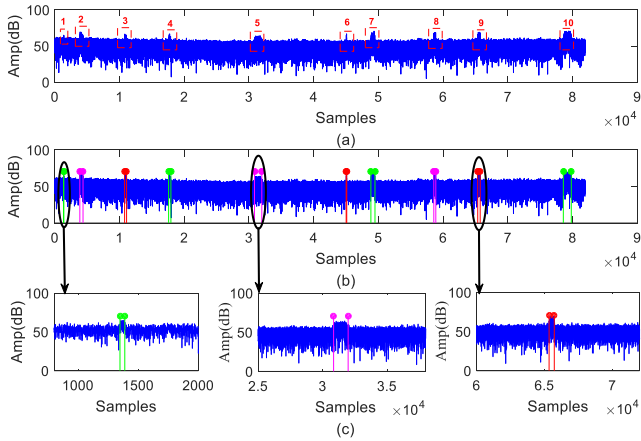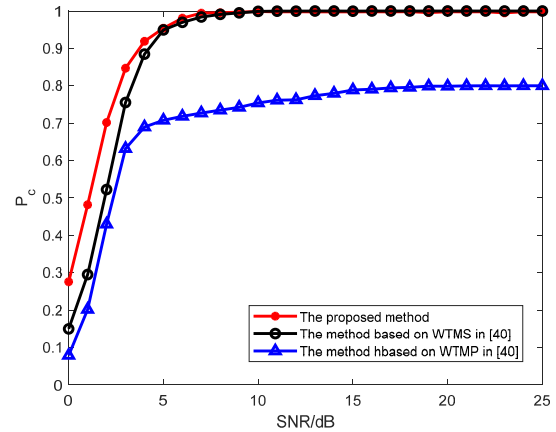
**FIGURE 12.** Detection results of the proposed detection algorithm: (a) The wideband spectrum; (b) The detected signals by the proposed algorithm; (c) The local of (b).

**TABLE 3.** The simulation parameter settings for simulating the algorithm performance at different SNRs.
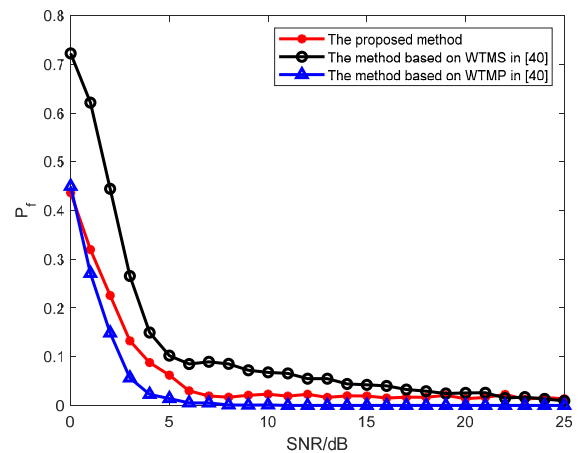
| | |
|---|---|
| Number of Monte Carlo for each SNR | 500 |
| Total detection bandwidth/ MHz | 60 |
| Number of signals | 10 |
| Signal frequencies/ MHz | Random, within [22 82] |
| Signal symbol rate/Ksps | Random, within [30 800] |
| SNR range/ dB | [0 25] |



**FIGURE 13.** The probability of detection versus SNR.



**FIGURE 14.** The probability of detecting spurious signals versus SNR.

to demonstrate the adaptability of the algorithm for detecting the narrowband and wideband signals simultaneously. It should be noted that the wavelet detection thresholds of signal detection algorithms based on WTMP and WTMS are set to the average of the wavelet transform multiscale sum and product, respectively. The energy based detection process after detecting the wavelet edges are adopted similar to the proposed algorithm. The performance comparisons are shown in Figure 13 and Figure 14.

Figure 13 shows the probability of detection $P_c$, given by (10). The proposed algorithm exhibits better detection performance among the whole SNR range compared to the signal detection algorithm based on WTMP. Although its detection performance is similar to that of the signal detection algorithm based on WTMS at SNRs above 5dB, it outperforms the signal detection algorithm based on WTMS at low SNRs 0-5dB. It demonstrates that the proposed algorithm meets the requirements of the narrowband and wideband signals detection at the same time well by applying the multiscale wavelet transform based edge detection. There is a contradiction in the detection of the narrowband signals and wideband signals for the signal detection algorithm based on WTMP. The local modulus maxima of the extra-narrowband signals are suppressed and miss-detected when the scale of multiplication is high as mentioned in [40]. This results in a decrease in the detection probability. The signal detection

algorithm based on WTMS overcomes the drawback of the WTMP algorithm through multiscale sum operation. So the signal detection algorithm based on WTMP has the lowest probability of detection, as shown in Figure 13.

The curve of the probability of detecting spurious signals $P_f$, given by (11) versus SNR is plotted in Figure 14. The signal detection approach based on WTMP gets the lowest probability of detecting spurious signals. The reason is spurious local modulus maxima induced by noise are random at each scale and could not propagate through the increase of wavelet scale, hence they are suppressed by multiscale multiplication operation. The signal detection algorithm based on WTMS has a similar suppressed effect on the noise-induced local modulus maxima by multiscale sum, but to a less extent compared with WTMP, especially at low SNRs. So the probability of detecting spurious signals is higher than that of the signal detection algorithm based on WTMP. It can be seen from Figure 14, the proposed algorithm has lower probability of detecting spurious signals compared with the signal detection algorithm based on WTMS. This is attributed to: 1) the signal detection strategy of combing the wavelet
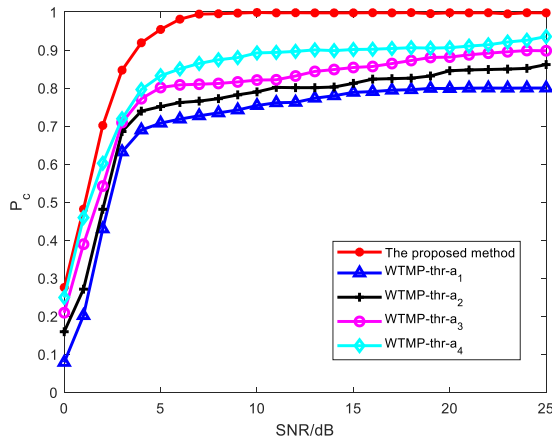
**FIGURE 15.** The detection probability performance comparison of the signal detection algorithm based on WTMP at different detection threshold values.
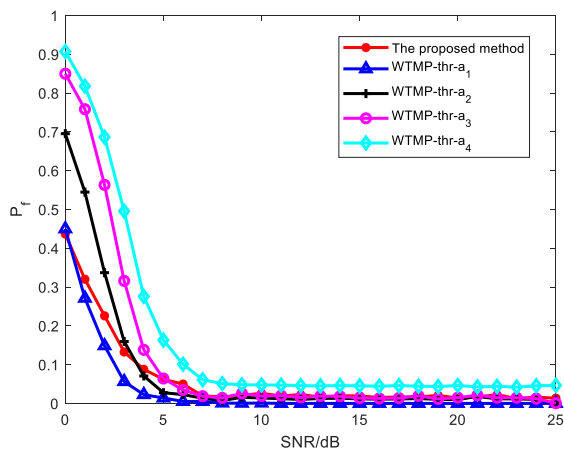


**FIGURE 16.** The probability of detecting spurious signals performance comparison of the signal detection algorithm based on WTMP at different detection threshold values.

transform local extreme detection with the spectrum energy detection at a single scale, which could effectively reduce the detection of false edges generated by noise; 2) the false detection of strong noises at the peak caused by the un-flat noise floor is solved by the morphological filtering; 3) Signal detection results at multiple scales are fused and eliminated selectively, further reduce the probability of spurious signal detection.

The performance of the signal detection algorithm based on WTMP is related to the setting of detection threshold value for local modulus maxima detection of WTMP. In theory, lowering the detection threshold value will increase the probability of detection. The detection threshold value is set to the average value of the wavelet transform multiscale product in the above simulation, expressed as $a_1$. We simulate the performances of the signal detection algorithm based on WTMP at lower detection threshold values $a_2 \sim a_4$ ($a_2 = 0.8a_1$, $a_3 = 0.5a_1$, $a_4 = 0.1a_1$). The performances of the signal detection algorithm based on WTMP at different detection threshold values are shown in Figures 15 and 16. From Figures 15 and

Figure 16, the probability of detecting spurious signals $P_f$ increases with the decrease of the wavelet detection threshold value, but the probability of detection $P_c$ can be improved to a certain extent. Compared with the proposed algorithm, it can be found that when the detection threshold value is reduced to $a_4$, the signal detection algorithm based on WTMP has a higher $P_f$ value than that of the proposed algorithm, but $P_c$ value is still lower than that of the proposed algorithm.

In summary, the performance of the proposed algorithm in rejecting spurious signals is better than the signal detection approach based on WTMS. Moreover, the proposed algorithm has obvious advantages over the signal detection method based on WTMP in the aspect of the probability of detection. From Figures 13 and 14, when the SNR is higher than 6dB, the detection probability of the proposed algorithm can reach more than 95% while the probability of spurious signal detection is less than 3%.

## IV. CONCLUSION

In this paper, a low false alarm and narrow-wide band compatible signal detection algorithm combining the multiscale wavelet transform extremum detection with the spectrum energy detection is proposed. It overcomes the drawback of the suppression of narrowband signals at high scales encountered in the wideband signal detection approach based on WTMP, at the same time it achieves a lower probability of detecting false signals compared with the wideband signal detection method based on WTMS. In summary, the proposed algorithm is able to achieve excellent narrow-wide band compatible detection performance while realizing a relatively low probability of detecting spurious signals. This algorithm can be applied in the spectrum monitoring, spectrum sensing of cognitive radio, and so on.

## REFERENCES

[1] B. Pascal and R. Bardenet, "A covariant, discrete time-frequency representation tailored for zero-based signal detection," *IEEE Trans. Signal Process.*, vol. 70, pp. 2950–2961, 2022.

[2] C.-I. Chang, "Hyperspectral anomaly detection: A dual theory of hyperspectral target detection," *IEEE Trans. Geosci. Remote Sens.*, vol. 60, 2022, Art. no. 5511720.

[3] T. Zuo, F. Wang, and J. Zhang, "Sparsity signal detection for indoor GSSK-VLC system," *IEEE Trans. Veh. Technol.*, vol. 70, no. 12, pp. 12975–12984, Dec. 2021.

[4] K. Adhikari and S. Kay, "An exact solution for sparse sampling for optimal detection of known signals in Gaussian noise," *IEEE Signal Process. Lett.*, vol. 30, pp. 369–373, 2023.

[5] S. Arya and Y. H. Chung, "Fault-tolerant cooperative signal detection for petahertz short-range communication with continuous waveform wideband detectors," *IEEE Trans. Wireless Commun.*, vol. 22, no. 1, pp. 88–106, Jan. 2023.

[6] Z. Chen, Y. Shi, Y. Wang, X. Li, X. Yu, and Y. Shi, "Unlocking signal processing with image detection: A frequency hopping detection scheme for complex EMI environments using STFT and CenterNet," *IEEE Access*, vol. 11, pp. 46004–46014, 2023.

[7] Y. Arjoune, Z. E. Mrabet, H. E. Ghazi, and A. Tamtaoui, "Spectrum sensing: Enhanced energy detection technique based on noise measurement," in *Proc. IEEE 8th Annu. Comput. Commun. Workshop Conf. (CCWC)*, Jan. 2018, pp. 828–834.

[8] F. Salahdine, H. E. Ghazi, N. Kaabouch, and W. F. Fihri, "Matched filter detection with dynamic threshold for cognitive radio networks," in *Proc. Int. Conf. Wireless Netw. Mobile Commun. (WINCOM)*, Oct. 2015, pp. 1–6.

[9] D. Cohen and Y. C. Eldar, "Compressed cyclostationary detection for cognitive radio," in *Proc. IEEE Int. Conf. Acoust., Speech Signal Process. (ICASSP)*, Mar. 2017, pp. 3509–3513.

[10] T. Haque, M. Bajor, Y. Zhang, J. Zhu, Z. A. Jacobs, R. B. Kettlewell, J. Wright, and P. R. Kinget, "A reconfigurable architecture using a flexible LO modulator to unify high-sensitivity signal reception and compressed-sampling wideband signal detection," *IEEE J. Solid-State Circuits*, vol. 53, no. 6, pp. 1577–1591, Jun. 2018.

[11] N. West, T. O'Shea, and T. Roy, "A wideband signal recognition dataset," in *Proc. IEEE 22nd Int. Workshop Signal Process. Adv. Wireless Commun. (SPAWC)*, Sep. 2021, pp. 6–10.

[12] Y. Yuan, Z. Sun, Z. Wei, and K. Jia, "DeepMorse: A deep convolutional learning method for blind Morse signal detection in wideband wireless spectrum," *IEEE Access*, vol. 7, pp. 80577–80587, 2019.

[13] M. O. Mughal and S. Kim, "Signal classification and jamming detection in wide-band radios using Naïve Bayes classifier," *IEEE Commun. Lett.*, vol. 22, no. 7, pp. 1398–1401, Jul. 2018.

[14] C. M. Spooner and A. N. Mody, "Wideband cyclostationary signal processing using sparse subsets of narrowband subchannels," *IEEE Trans. Cognit. Commun. Netw.*, vol. 4, no. 2, pp. 162–176, Jun. 2018.

[15] J. A. Sheikh, Z. I. Mir, M. U. A. Mufti, S. A. Parah, and G. M. Bhat, "A new filter bank multicarrier (FBMC) based cognitive radio for 5G networks using optimization techniques," *Wireless Pers. Commun.*, vol. 112, no. 2, pp. 1265–1280, May 2020.

[16] K. Sharma and A. Sharma, "Design of cosine modulated filter banks exploiting spline function for spectrum sensing in cognitive radio applications," in *Proc. IEEE 1st Int. Conf. Power Electron., Intell. Control Energy Syst. (ICPEICES)*, Jul. 2016, pp. 1–5.

[17] I. Raghu, S. S. Chowdary, and E. Elias, "Efficient spectrum sensing for cognitive radio using cosine modulated filter banks," in *Proc. IEEE Region Conf. (TENCON)*, Nov. 2016, pp. 2086–2089.

[18] J. N. Javed, M. Khalil, and A. Shabbir, "A survey on cognitive radio spectrum sensing: Classifications and performance comparison," in *Proc. Int. Conf. Innov. Comput. (ICIC)*, Nov. 2019, pp. 1–8.

[19] Z. Qin, J. Fan, Y. Liu, Y. Gao, and G. Y. Li, "Sparse representation for wireless communications: A compressive sensing approach," *IEEE Signal Process. Mag.*, vol. 35, no. 3, pp. 40–58, May 2018.

[20] S. K. Sharma, E. Lagunas, S. Chatzinotas, and B. Ottersten, "Application of compressive sensing in cognitive radio communications: A survey," *IEEE Commun. Surveys Tuts.*, vol. 18, no. 3, pp. 1838–1860, 3rd Quart., 2016.

[21] F. Salahdine, N. Kaabouch, and H. El Ghazi, "A survey on compressive sensing techniques for cognitive radio networks," *Phys. Commun.*, vol. 20, pp. 61–73, Sep. 2016.

[22] Z. Li, W. Xu, X. Zhang, and J. Lin, "A survey on one-bit compressed sensing: Theory and applications," *Frontiers Comput. Sci.*, vol. 12, no. 2, pp. 217–230, Apr. 2018.

[23] Y. Vasavada and C. Prakash, "Sub-Nyquist spectrum sensing of sparse wideband signals using low-density measurement matrices," *IEEE Trans. Signal Process.*, vol. 68, pp. 3723–3737, 2020.

[24] T. Guo, T. Zhang, E. Lim, M. López-Benítez, F. Ma, and L. Yu, "A review of wavelet analysis and its applications: Challenges and opportunities," *IEEE Access*, vol. 10, pp. 58869–58903, 2022.

[25] S. Mallat and W. L. Hwang, "Singularity detection and processing with wavelets," *IEEE Trans. Inf. Theory*, vol. 38, no. 2, pp. 617–643, Mar. 1992.

[26] S. Mallat and S. Zhong, "Characterization of signals from multiscale edges," *IEEE Trans. Pattern Anal. Mach. Intell.*, vol. 14, no. 7, pp. 710–732, Jul. 1992.

[27] J. Liu, E. M. Enderlin, H.-P. Marshall, and A. Khalil, "Automated detection of marine glacier calving fronts using the 2-D wavelet transform modulus maxima segmentation method," *IEEE Trans. Geosci. Remote Sens.*, vol. 59, no. 11, pp. 9047–9056, Nov. 2021.

[28] Z. Lv, G. Wang, Z. Wang, H. Zhao, and W. Gao, "Application of weld scar recognition in small-diameter transportation pipeline positioning system," *Electronics*, vol. 11, no. 7, p. 1100, Mar. 2022.

[29] T. Lan, H. Xiao, Y. Li, and J. Chen, "Enhanced current differential protection for HVDC grid based on Bergeron model: A parameter error tolerable solution," *IEEE Trans. Power Del.*, vol. 36, no. 3, pp. 1869–1881, Jun. 2021.

[30] C. Zhou, K. Guo, B. Yang, H. Wang, J. Sun, and L. Lu, "Singularity analysis of cutting force and vibration for tool condition monitoring in milling," *IEEE Access*, vol. 7, pp. 134113–134124, 2019.

[31] Z. Tian and G. B. Giannakis, "A wavelet approach to wideband spectrum sensing for cognitive radios," in *Proc. 1st Int. Conf. Cognit. Radio Oriented Wireless Netw. Commun.*, Jun. 2006, doi: 10.1109/CROWN-COM.2006.363459.

[32] A. Kumar, S. Saha, and R. Bhattacharya, "Wavelet transform based novel edge detection algorithms for wideband spectrum sensing in CRNs," *AEU Int. J. Electron. Commun.*, vol. 84, pp. 100–110, Feb. 2018.

[33] S. Charaâ and N. Ellouze, "Multiscale product Riesz wavelet for color edge detection in Hilbert domain," in *Proc. Eur. Modeling Symp.*, Oct. 2014, pp. 215–220.

[34] Z. Moussavi, D. Flores, and G. Thomas, "Heart sound cancellation based on multiscale products and linear prediction," in *Proc. 26th Annu. Int. Conf. IEEE Eng. Med. Biol. Soc.*, Sep. 2004, pp. 3840–3843.

[35] T. Pan, J. Chen, Z. Zhou, C. Wang, and S. He, "A novel deep learning network via multiscale inner product with locally connected feature extraction for intelligent fault detection," *IEEE Trans. Ind. Informat.*, vol. 15, no. 9, pp. 5119–5128, Sep. 2019.

[36] Y. Cheng, X. Zhang, X. Wang, and J. Li, "Battery state of charge estimation based on composite multiscale wavelet transform," *Energies*, vol. 15, no. 6, pp. 1–16, 2022.

[37] J.-L. Meng, L. Jin, Q. Pan, and H.-C. Zhang, "MSE analyses of thresholding by multiscale product," in *Proc. Int. Conf. Wavelet Anal. Pattern Recognit.*, Nov. 2007, pp. 891–896.

[38] Z. Xiaoli, "Edge detection algorithm based on multiscale product with Gaussian function," *Proc. Eng.*, vol. 15, pp. 2650–2654, Jan. 2011.

[39] S. Jindal, D. Dass, and R. Gangopadhyay, "Wavelet based spectrum sensing in a multipath Rayleigh fading channel," in *Proc. 20th Nat. Conf. Commun. (NCC)*, Feb. 2014, pp. 1–6.

[40] Y.-L. Xu, H.-S. Zhang, and Z.-H. Han, "The performance analysis of spectrum sensing algorithms based on wavelet edge detection," in *Proc. 5th Int. Conf. Wireless Commun., Netw. Mobile Comput.*, Sep. 2009, pp. 1–4.

[41] S. Vadrevu and M. S. Manikandan, "A robust pulse onset and peak detection method for automated PPG signal analysis system," *IEEE Trans. Instrum. Meas.*, vol. 68, no. 3, pp. 807–817, Mar. 2019.

[42] K. Zhang, F. Zhang, Z. Feng, J. Sun, and Q. Wu, "Fusion of panchromatic and multispectral images using multiscale convolution sparse decomposition," *IEEE J. Sel. Topics Appl. Earth Observ. Remote Sens.*, vol. 14, pp. 426–439, 2021.

[43] S. E. El-Khamy, M. S. El-Mahallawy, and E. S. Youssef, "Improved wideband spectrum sensing techniques using wavelet-based edge detection for cognitive radio," in *Proc. Int. Conf. Comput., Netw. Commun. (ICNC)*, Jan. 2013, pp. 418–423.

[44] G. Hattab and M. Ibnkahla, "Multiband spectrum access: Great promises for future cognitive radio networks," *Proc. IEEE*, vol. 102, no. 3, pp. 282–306, Mar. 2014.

[45] Y. Zeng, Y.-C. Liang, and M. W. Chia, "Edge based wideband sensing for cognitive radio: Algorithm and performance evaluation," in *Proc. IEEE Int. Symp. Dyn. Spectr. Access Netw. (DySPAN)*, May 2011, pp. 538–544.

• • •